coatings

MDPI

Article

Analysis of the Possibility of Using New Types of Protective Coatings and Abrasion-Resistant Linings under the Operating Conditions of the Spiral Classifier at KGHM Polska Miedź S.A. Ore Concentration Plant

Marcin Czekajło [1,*], Krzysztof Zakowski [2], Stefan Krakowiak [2] and Sławomir Kierepa [1]

[1] KGHM Polska Miedź S.A. Ore Concentration Plant, 1 Kopalniana Street, 59-101 Polkowice, Poland; slawomir.kierepa@kghm.com
[2] Faculty of Chemistry, Department of Electrochemistry, Corrosion and Materials Engineering, Gdansk University of Technology, 11/12 Gabriela Narutowicza Street, 80-233 Gdansk, Poland; krzysztof.zakowski@pg.edu.pl (K.Z.); stefan.krakowiak@pg.edu.pl (S.K.)
* Correspondence: marcin.czekajlo@kghm.com

Abstract: A study was carried out to select the appropriate coatings for corrosion protection of the spiral classifier working at KGHM Polska Miedź S.A. Ore Concentration Plant. The abrasion resistance of selected protective coatings and wear-resistant linings was investigated using a DT-523 rotary abrasion tester with Taber CS-10 rubber abrasive discs. The average weight loss of the coatings after a cycle of 2000 revolutions was determined. Tests of protective coatings using the electrochemical impedance spectroscopy (EIS) technique were carried out to determine the suitability of coatings in the highly saline environment of the aqueous suspension of ground copper ore. During the measurements, changes in resistance, polarising current and capacitance were determined as a function of time for the tested coatings. The linings selected on the basis of laboratory tests were also tested under industrial conditions. Their degrees of wear were characterised. The results obtained indicated the highest abrasion resistance of materials from the polyolefin group (polyethylenes), where the average weight loss did not exceed 5 g/dm^2. In the case of protective coatings, the highest durability was demonstrated by coatings with additives of ceramic aggregates, phenol-epoxy, and an elastomeric coating based on polyurea, whose average weight loss during the test cycle did not exceed 19 g/dm^2. EIS measurements showed that the tested coatings were resistant to the aggressive environment of the feedstock. Tests under cathodic polarisation conditions of the samples at a potential below the protection potential showed that they were resistant to a highly saline environment and were also resistant to its alkalinisation resulting from the application of cathodic protection, which will be used to protect the classifier together with protective coatings. Tests carried out under industrial conditions using wear-resistant linings made of plastics have made it possible to analyse the mechanism and degree of wear of the various materials during the operation of the classifier. Measurements of lining wear were made in relation to baseline volumes. Polyurethane, a polymer lining based on MDI and PTMG, and those made of ultra-high-molecular-weight polyethylene with anti-stick additives showed the lowest wear rates.

Keywords: corrosion-erosion; spiral classifier; paint coatings; wear-resistant linings; rotational wear tester; wear resistance tests; electrochemical impedance spectroscopy (EIS)

check for updates

Citation: Czekajło, M.; Zakowski, K.; Krakowiak, S.; Kierepa, S. Analysis of the Possibility of Using New Types of Protective Coatings and Abrasion-Resistant Linings under the Operating Conditions of the Spiral Classifier at KGHM Polska Miedź S.A. Ore Concentration Plant. *Coatings* **2021**, *11*, 1138. https://doi.org/10.3390/coatings11091138

Academic Editor: Alina Pruna

Received: 19 August 2021
Accepted: 15 September 2021
Published: 19 September 2021

Publisher's Note: MDPI stays neutral with regard to jurisdictional claims in published maps and institutional affiliations.

Copyright: © 2021 by the authors. Licensee MDPI, Basel, Switzerland. This article is an open access article distributed under the terms and conditions of the Creative Commons Attribution (CC BY) license (https://creativecommons.org/licenses/by/4.0/).

1. Introduction

The Ore Concentration Plant (O/ZWR) is an independent unit in the organisational structure of KGHM Polska Miedź S.A., comprising three production regions: Lubin, Polkowice and Rudna. It plays a key role in the copper ore processing sequence. The primary task of O/ZWR is to maximise metal yields and produce concentrates with the quality parameters required by steel plants, at the lowest possible cost [1,2].

The ore extracted from the mines of KGHM Polska Miedź S.A. contains, on average, about 1.52% of useful metal [3]. Valuable ore is subjected to processing, the main operation of which is enrichment by flotation [4–7]. As a result of this operation, a concentrate is obtained with a copper content enabling it to be metallurgically processed in the smelting process. Part of the excavated material with a low metal content is flotation waste, which is transported to the tailings pond named Żelazny Most [8]. The technology used in the O/ZWR allows for the effective recovery of copper, silver and other elements from the extracted ore. This is evidenced by high recovery of these metals (up to approximately 90%) and an average copper content in concentrates of 23% with a simultaneous high level of ore processing oscillating around 33 million tonnes of wet weight [9].

The technological operations carried out in O/ZWR require maintaining high availability indicators for machinery and equipment and technical installations. One of the main reasons for their reduced efficiency is the operation under severe corrosion-erosion conditions [10].

Corrosion is the process of destroying materials as a result of electrochemical reactions, while erosion is mechanical destruction. The simultaneous occurrence of corrosion and erosion in an aqueous environment is known as erosion corrosion (EC). The speed of the EC process can be much higher than the sum of the rates of the separate processes. This is called positive synergism—increasing the rate of corrosion by erosion, or enhancing erosion by corrosion [11,12].

An inspection of the classifier systems in O/ZWR showed the need for effective methods of corrosion protection for classifiers [13,14]. For this reason, the development of technology for the anticorrosion protection of classifiers is based on research on the possibility of increasing the effectiveness of anticorrosion protection in grinding-classifier systems by creating conditions for the cooperation of coating protection and wear-resistant linings collaborating additionally with cathodic protection [15,16].

Polymer coatings, whose role is to protect steel structures against corrosion, are most exposed to plastic or elastic stresses arising during operation. Plastic deformation may arise only after exceeding the elastic limit, which, excluding environmental conditions, may be caused by excessive (for a polymer coating) kinetic impact energy. Another possibility is that micro-cutting can occur when the tangential forces to the coating surface are sufficient. An important feature in the course of this process is the hardness of both the factor (dust, stones, sludge, lumps of earth, sand, ice, etc.) and the polymer [17].

Corrosion-erosion phenomena may occur on the working surfaces of the spiral where there is continuous contact (friction) with the ground feed (Figure 1). The research is therefore focused on protective materials in the form of paint coatings and wear-resistant linings.

Figure 1. View of a working two-winding classifier.

The process of segregation of feed grains in terms of their size and weight in the water medium is carried out in spiral classifiers and hydrocyclones [18–22]. There are 29 parallel grinding and classifying systems in O/ZWR, comprising 86 mills and 29 classifiers, each equipped with two spirals, making a total of 58 units. A schematic of the grinding and classifying system is shown in Figure 2 and the basic specifications of the classifier in Table 1.

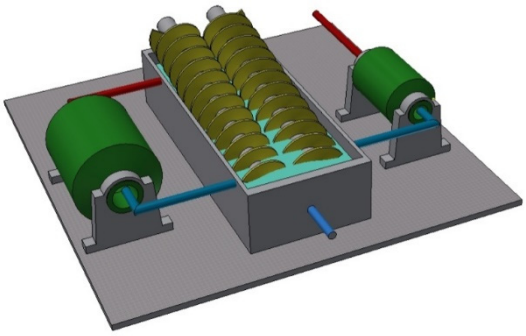

Figure 2. Illustrative diagram of a grinding and classification system. Spatial view. A first grinding (throughput) mill, a classifier and a second grinding mill.

Table 1. Basic technical data and performance of the selected spiral classifier.

Dimensions (Length × Width × Height) (m)	9.82 × 5.13 × 4.02
Classifier Inclination Angle (°)	19
Diameter of Spirals (mm)	Ø 2400
Spiral Speed (1/min)	3.5
Maximum Underflow Capacity (Mg/h)	250
Density of Feed (g/dm^3)	1500–1650
Overflow Density (g/dm^3)	1350–1450
Underflow Density (g/dm^3)	2000–2200

The working environment of spiral classifiers is an aqueous suspension of ground copper ore, 95% of whose grain size is less than 1 mm. The excavated material sent to the process consists of three main lithological fractions: shale, dolomite and sandstone, whose average shares in 2020 were 9.83%, 60.70% and 29.47%, respectively. The water used in the technological process comes from the Żelazny Most tailings pond (83%) and water from mine drainage (17%). Data for 2020, coming from the monitoring system for chlorides and sulphates created for KGHM Polska Miedź S.A., show the presence of chloride ions (Cl^-) at the level of 37.6 g/dm^3, which, together with underground waters, go to the Polkowice area, 1.43 g/dm^3 to the Lubin area and 120.60 g/dm^3 to the Rudna area. In the case of backwaters from the tailings pond Żelazny Most, the chloride (Cl^-) concentration is close to 36.8 g/dm^3.

Sulphate ions SO_4^{2-} are also another component of water-soluble salts. Their present concentration in mine waters directed to the Polkowice area is 1.67 g/dm^3, to the Lubin area, 0.96 g/dm^3 and to the Rudna area, 2.43 g/dm^3, while the backwaters from the tailings pond Żelazny Most contain about 3.4 g/dm^3 of SO_4^{2-} ions. The concentration of sulphate in waters directed to O/ZWR has remained at a similar level for many years and slightly exceeds 3.0 g/dm^3. The above components cause the process water to be characterised by a very high corrosion aggressiveness [23], and it is necessary to protect the process equipment against corrosion.

The aim of this work was to carry out research to select coatings that could be used in an industrial setting to protect the steel spirals of double-strand classifiers grading copper ore previously subjected to a grinding process. To the authors' knowledge, this type of solution is not used for similar facilities in the ore mining and concentration industry. The

combined use of coatings and cathodic protection of the classifier is being designed [15], which will be a technological innovation. The research results presented in this paper may be useful for those designing the protection of various industrial facilities that are exposed to the combined erosive and corrosive effects of highly saline environments.

2. Materials and Methods

Testing of the selected materials was carried out in two groups: plastics and protective coatings. In addition, ordinary uncoated structural steel, which is the backbone-substrate for the installation of the classifier spiral linings, was tested as a comparative benchmark. These material groups included eleven plastic samples, six paint samples and one sample made of ordinary structural steel (Table 2). For all materials, three samples each were prepared, applied to a substrate of S235 structural steel, measuring 10 × 10 cm and 3 mm thick. The tests were conducted in accordance with EN ISO 7784-2:2016-05 [24]. Taber CS-10 abrasive discs (TABER® Industries, North Tonawanda, NY, USA) and a load of 10 N per tester arm were used.

Table 2. Summary of materials tested for abrasion resistance.

Sample Number	Type of Material
Group of Materials	
A	Epoxy system with alumina ceramic filling
B	Polyurethane
C	Ultra-high molecular-modified polyethylene with antiadhesive additives
D	Polymer based on MDI (methylene diphenyl diisocyanate) and PTMG (polytetramethylene glycol)
E	Polyurethane elastomer
F	PA 6 C (cast polyamide 6) with added molybdenum disulphide
G	PA 6 C (polyamide 6 cast)
H	High-density polyethylene
I	Epoxy system with ceramic filling
J	Rubber-like urethane mass
K	Vulcanised rubber
Coating Group	
L	Amine-cured phenol-epoxy coating
M	Elastomeric coating based on pure polyurea primed with epoxy coating
N	Epoxy coating with ceramic filling
O	Coating consisting of hard and dense ceramic aggregates and a polymer bonding agent
P	Epoxy coating with 100% solids content
R	Two-component epoxy resin-based coating
Structural Steel	
S	Sheet metal S 235

Prior to testing, central holes were drilled to accommodate the specimens and the size and weight of the specimens were checked to ensure that they met technical requirements, reducing them by machining if necessary.

2.1. Determination of Abrasion Resistance of Protective Coatings and Wear Linings—Laboratory Tests

2.1.1. Mass Measurement of Coating Samples

Samples whose size (distance of the edge of the sample from the central hole could not be more than 7.5 cm) or weight (maximum weight of 210 g resulting from the measuring range of the balance used) exceeded the equipment capabilities of the testing apparatus were prepared for the test by mechanical treatment: machining, drilling or grinding.

The masses of samples L, M and N were measured using an analytical balance FA2104 (Yuyao Beyond Dream Commerce Co., Ltd., Zhejiang, China) with an accuracy of 0.1 mg. Samples O, P and R were weighed on a mass comparator with an accuracy of 10 mg due to the significant excess of allowable mass.

MOST WIEDZY Downloaded from mostwiedzy.pl

2.1.2. Measuring the Thickness of Tested Coating Samples

The coating thickness on metal-backed samples was measured with reference to EN ISO 2808:2020-01 [25]. An ElektroPhysik MiniTest 735 m was used for the measurements. The results of the measurements are shown in Table 3. The thickness of the individual coatings was determined by the manufacturers and adapted to the operating conditions of the spiral classifier.

Table 3. Results of thickness measurements of coatings with metal substrates.

Type of Sample	Sample Photo	Sample Mark	Measurement 1 (µm)	Measurement 2 (µm)	Measurement 3 (µm)	Average Thickness (µm)	Standard Deviation (µm)
Coat L	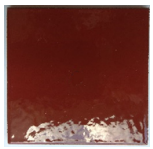	1	610	593	624	609	13
		2	694	696	666	685	14
		3	642	630	644	639	6
Coat M		1	3030	2920	3300	3083	160
		2	3200	2995	2820	3005	155
		3	3550	3390	3570	3503	81
Coat N	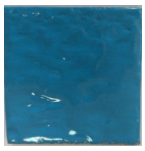	1	848	548	644	680	125
		2	638	551	666	618	49
		3	812	1202	1210	1075	186
Coat O		1	7290	6610	6140	6680	472
		2	7730	7630	6180	7180	708
		3	8680	8390	8530	8533	118
Coat P		1	1202	1292	1190	1228	46
		2	1100	1106	1134	1117	15
		3	1156	986	1148	1097	78
Coat R		1	634	560	533	576	43
		2	554	680	642	625	53
		3	520	550	506	525	18

2.1.3. Research Methodology

The test was carried out on a device called a DT-523 rotational abrasion tester (Agencja ANTICORR Gdańsk Sp. z o.o., Gdańsk, Poland) using Taber CS-10-type rubber abrasive discs. For all types of coatings and plastics, 500 preliminary rotations were performed to level the abrasive surface, after which the samples were weighed, taking the indicated weight as the initial weight. This was followed by 2000 rotations each, with samples removed and weighed and abrasive discs cleaned every 500 rotations. The load was 10 N per arm and the number of rotations per minute was 60. Samples numbered O, P and R due to exceeding a mass of 210 g were weighed only in the initial state and after a series of 2000 rotations.

MOST WIEDZY Downloaded from mostwiedzy.pl

2.2. Determination of Resistance of Coatings by Electrochemical Impedance Spectroscopy (EIS)—Laboratory Testing

The resistance of coatings to the environment present in spiral classifiers described in the introduction of this paper was carried out by electrochemical impedance spectroscopy (EIS) for the coating samples designated as L, M, N, O, P and R, which are listed in Table 3. Sycopel's Specstat kit (Sycopel Scientific Ltd, Washington (Tyne and Wear), UK) with a high-impedance ATLAS attachment (Atlas Sollich, Gdańsk, Poland) was used for the tests. The tests were carried out in a two-electrode system, where the working electrode was steel covered with a suitable organic coating and the counter-electrode was a platinum grid. The perturbation signal was a sinusoid with an amplitude of 150 mV. Tests were carried out in the frequency range from 10 kHz to 1 Hz. A feed taken from a spiral classifier from the Polkowice production area was used as the electrolyte in the study. After analytical testing, the presence of 35.8 g of Cl^-/dm^3 was found. The first measurement was taken after 24 h of exposure of the coatings to the aggressive environment. Measurements were repeated every 30 days.

The optimisation program ZSimpWin (V3.10) was used to evaluate the results of the study. As none of the samples tested showed degradation at the level of coating failure and the start of corrosion processes on the steel substrate, the electrical-equivalent circuit [26] shown in Figure 3 was used for the analyses.

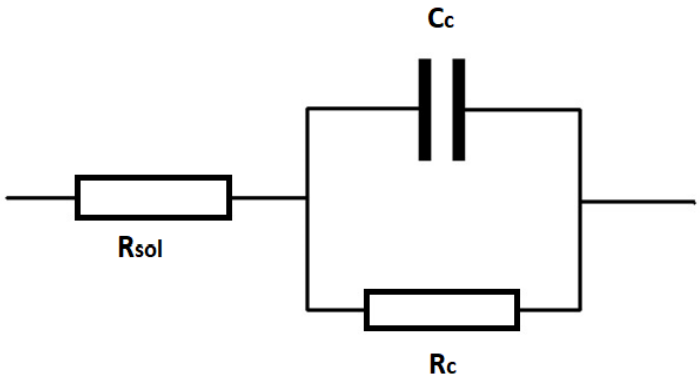

Figure 3. Electrical equivalent circuit diagram: Rsol—electrolyte resistance; Rc—coating resistance; Cc—coating capacitance.

The results are presented in the form of the dependence of the changes in resistance and capacitance of coatings during exposure.

In addition to the good resistance to the highly corrosive and erosive environment of the feedstock, the coatings included in the tests are to cooperate with cathodic protection, so tests were also carried out to check whether the phenomena accompanying cathodic protection (alkalisation of the environment in the vicinity of the structure and hydrogen release in the event of possible overprotection near the polarisation anodes—"overprotection") do not adversely affect the condition of the coatings. For this purpose, circular defects were made on the coatings to the steel substrate with a diameter of 1 cm. PVC cups were glued onto the surface of the shells and filled with the feed. A platinised titanium-polarising electrode and an Ag/AgCl reference electrode were also inserted into each dish. After 1 h, the corrosion potentials of the steels were measured and then the test systems were connected to a potentiostat, which maintained the cathodic polarisation of the samples to a potential of −1.1 V vs. Ag/AgCl. During the exposure, changes in the polarising current flowing in the test system were monitored. The prepared samples were left for 30 days and, after this time, the current and the potential of the steel substrate were measured. After a further 30 days, the measurements were repeated and the surfaces of the stripped steel and the immediate surrounding area were analysed to check for any reduction in adhesion of the coating to the substrate.

2.3. Determination of Abrasion Resistance of Wear-Resistant Linings—Industrial Tests

Six materials were selected for testing under industrial conditions, including polyurethane, ultra-high-molecular-weight modified polyethylene with anti-adhesion additives, a polymer based on MDI and PTMG, cast polyamide 6, cast polyamide 6 with the addition of molybdenum disulphide, and high-density polyethylene. The criterion for selecting materials for the test was the abrasion resistance test results obtained previously.

The test linings were made in a shape mimicking the outer section of the classifier spiral, allowing the lining to be mounted on the spiral. The tested linings of the shape shown in Figure 4 can be divided into two groups due to their construction. The first had internal cores made of 8 mm-thick structural sheet metal. The purpose of the core fused into the lining was to stiffen it. This group includes polyurethane and polymeric linings based on MDI and PTMG. The second group was coreless linings (Figure 5), whose stiffness did not require additional reinforcements. This group of materials was made by mechanical processing, i.e. milling and drilling.

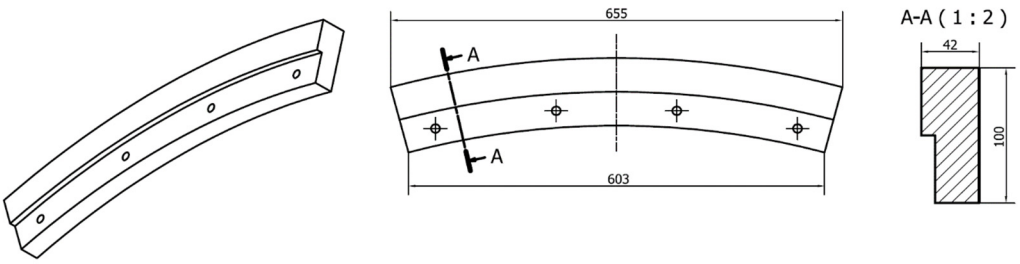

Figure 4. Spiral classifier edge lining—technical drawing (Dimensions in millimetres).

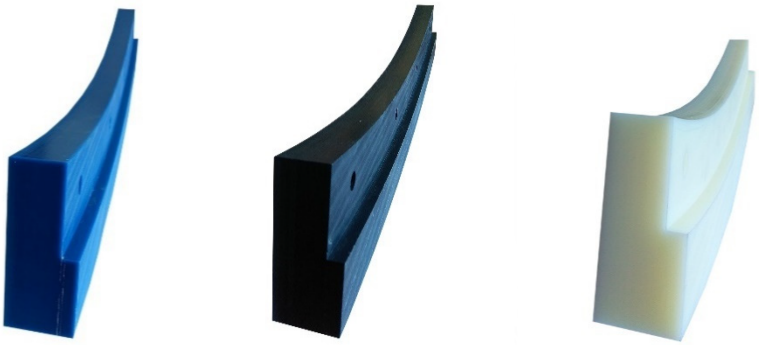

Figure 5. Selected test spiral classifier linings—ready for installation.

The base (comparison) lining was the current polyurethane lining. The tested linings were exposed under normal operating conditions of the spiral classifier (Figure 6).

Figure 6. View of the installed test linings—before starting the test.

MOST WIEDZY Downloaded from mostwiedzy.pl

The duration of the test was set at 10 months. During this time, the classifier with technology number K-211 worked 6387 h, while the average working time of one classifier working in the Polkowice area in 2020 was nearly 7500 h. During this period, an estimated 90,5850 Mg of dredged material in the form of an aqueous slurry with a density from 1500 to 1650 g/dm^3 was directed to the classifier, of which approximately 500,000 Mg was transported through the classifier linings, including test linings, towards the spillway.

3. Results and Discussion

3.1. Determination of Abrasion Resistance of Protective Coatings and Wear Linings—Laboratory Tests

Tests of coatings and linings showed differences in the abrasion resistance of the different materials. The surface view of the tested samples after abrasion testing is shown in Figures 7–12. The nominal dimensions of all samples shown in Figures 7–12 are 10 × 10 cm.

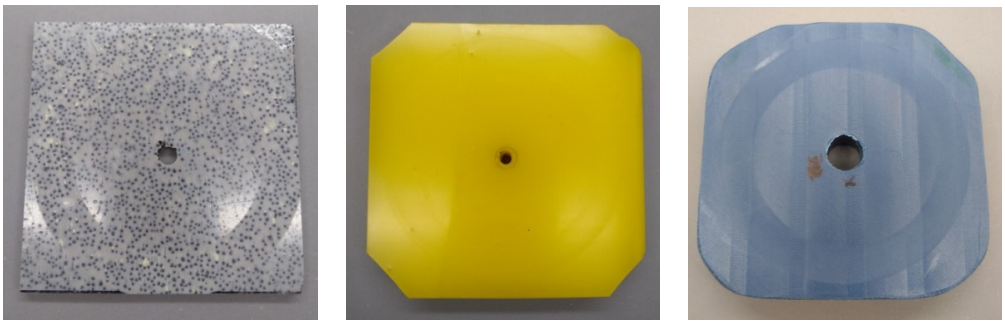

(**a**) (**b**) (**c**)

Figure 7. Samples (**a**): A, (**b**): B and (**c**): C after testing.

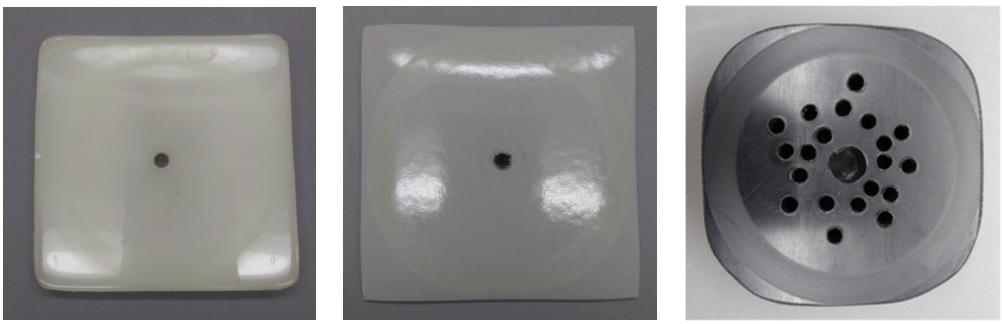

(**a**) (**b**) (**c**)

Figure 8. Samples (**a**): D, (**b**): E and (**c**): F after testing.

(**a**) (**b**) (**c**)

Figure 9. Samples (**a**): G, (**b**): H and (**c**): I after testing.

MOST WIEDZY Downloaded from mostwiedzy.pl

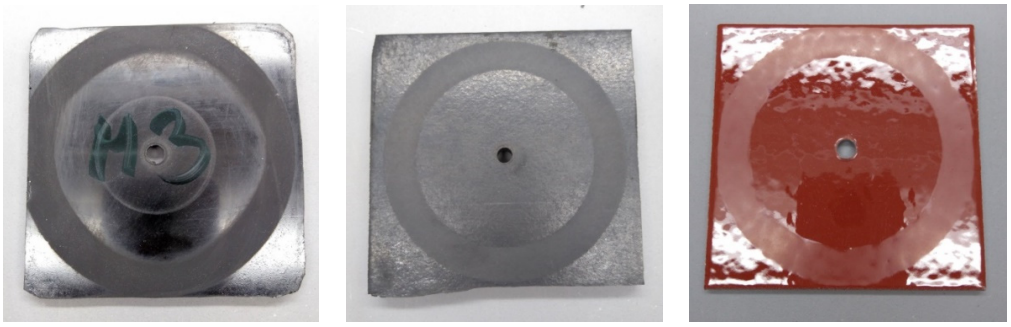

(**a**) (**b**) (**c**)

Figure 10. Samples (**a**): J, (**b**): K and (**c**): L after testing.

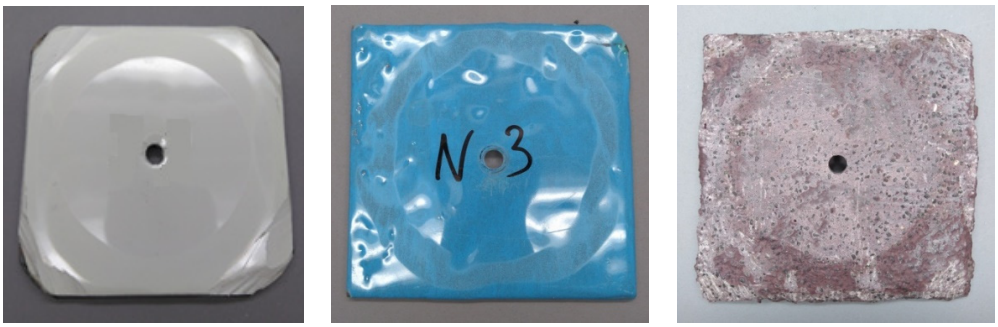

(**a**) (**b**) (**c**)

Figure 11. Samples (**a**): M, (**b**): N and (**c**): O after testing.

(**a**) (**b**) (**c**)

Figure 12. Samples (**a**): P, (**b**): R and (**c**): S after testing.

The abrasion resistance results obtained are presented as the weight loss of the samples after 2000 rotations (before which 500 rotations were carried out to even out the abrasion surface). For samples numbered D1–3 (Figure 10) and E1–3 (Figure 11), no loss was observed, which was most probably caused by the penetration of abrasive particles into the structure of the samples.

Tests carried out on the DT-523 rotary abrasion tester showed differences in the abrasion resistance of the different materials, as shown in Figures 13 and 14. When considering the samples from the plastics group, two main conclusions can be drawn. The first indicates that the lowest weight losses were achieved by samples C and H. Both samples were ultra-high-molecular-weight polyethylenes.

MOST WIEDZY Downloaded from mostwiedzy.pl

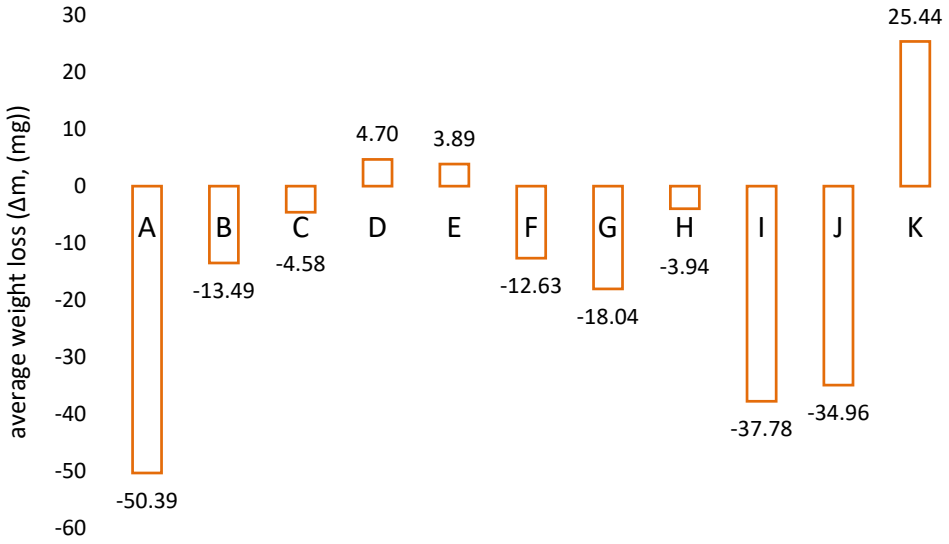

Figure 13. Average weight loss for the samples in the plastics group after a cycle of 2500 revolutions (initial and sequential) obtained with a DT-523 rotary abrasion tester.

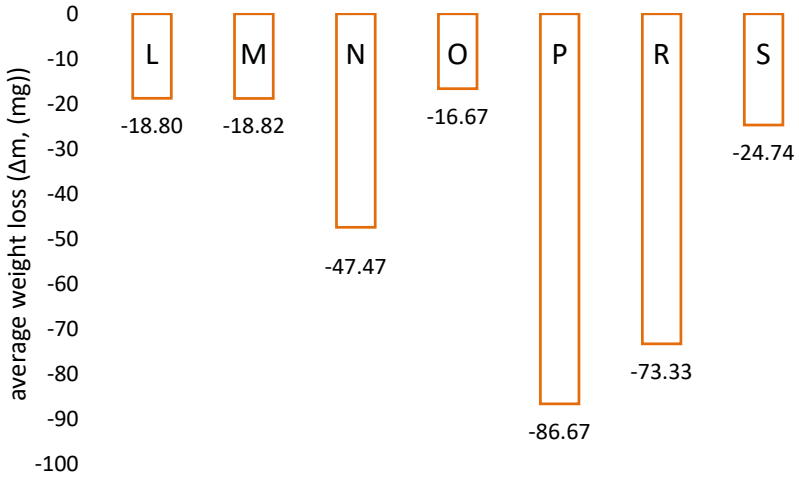

Figure 14. Average weight loss for the coating group and structural steel specimens after a cycle of 2500 rotations (initial and sequential) obtained on a DT-523 rotary abrasion tester.

A further observation indicates that samples D, E and K achieved a weight gain, which was most likely due to particles from the abrasive disc penetrating the plastic structure (Figure 13). On the samples, a greenish tarnish could be observed on the abraded surface.

Among the coatings and structural steel group, three samples with similar weight losses can be observed, i.e., L, M and O, which do not exceed 20 mg after a cycle of 2500 revolutions, as shown in Figure 14. In this group, the most durable coatings were those containing hard additives of ceramic aggregates, phenolic-epoxy and elastomeric coatings based on polyurethane. Other samples tested achieved weight losses of up to nearly 90 mg. It should be noted that ordinary S 235 structural steel lost nearly 25 mg during the entire test cycle.

Comparing the obtained test results, it should be stated that the highest durability during the conducted tests of abrasion resistance was obtained for samples marked as C and H, i.e. samples from the group of polyolefins (polyethylenes), i.e. materials consisting mainly of carbon and hydrogen. Additives supplementing the material composition of tested samples are trade secrets of the manufacturers. Paint coatings designated as L, M and O also achieved a satisfactory result; however, the losses in their masses were more than four times higher compared to materials made of polyethylene.

3.2. Determination of Resistance of Coatings by Electrochemical Impedance Spectroscopy (EIS)—Laboratory Testing

The first measurement, taken two days after the start of exposure, indicates that all tested coatings showed very good barrier properties. During the exposure, none of the tested systems showed a decrease in impedance below the value considered as the limit, i.e., 10^6 Ω. The dynamics of resistance and film capacitance changes were different for the tested coatings. This is due to both the performance properties of the coatings, as well as the varying thicknesses [27,28]. Figure 15 shows example impedance spectra in the form of Nyquist plots obtained for one of the organic coatings tested. Table 4 presents the results of the calculations of the resistance and the capacity of the coating fitted to the equivalent model shown in Figure 3 together with the estimated measurement error.

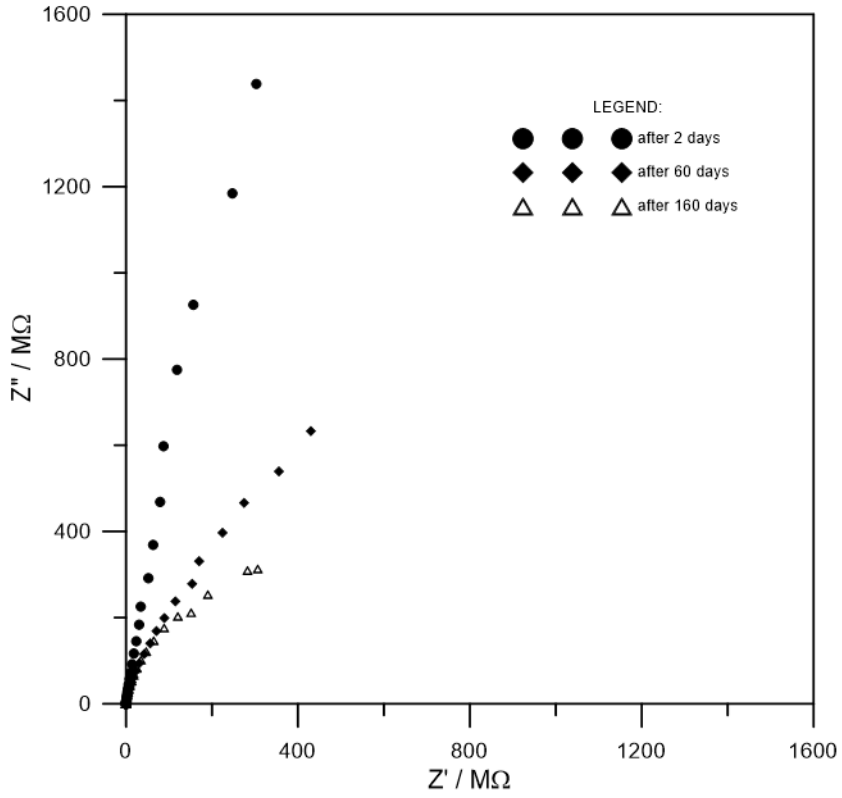

Figure 15. Example impedance spectra obtained for a selected organic coating (coating "P").

Table 4. The results of the calculation of the resistance and capacity of the coating.

Expousure time/measurement error	**Rc/Ω**	**Cc/F**
After 2 days	8.79×10^9	8.88×10^{-10}
Relative standard error/%	24.01	0.33
After 60 days	6.02×10^8	1.19×10^{-9}
Relative standard error/%	6.24	0.47
After 160 days	1.25×10^8	6.62×10^{-9}
Relative standard error/%	10.23	5.61

The results for the other tested coatings are presented as the relationship $R_C = f(t)$ and $C_C = f(t)$ (Figure 16). The typical behaviour of coatings exposed in aggressive environments was evident. There was then an initial drop in the resistance of the coatings, followed by stabilisation at high or very high resistance values, reaching levels ranging from 10,000 MΩ

MOST WIEDZY Downloaded from mostwiedzy.pl

for the M coating to around 55,000 MΩ for the O coating. This is related, among other things, to the recommended thickness of the coatings that have been specified to protect the surfaces of spiral classifiers.

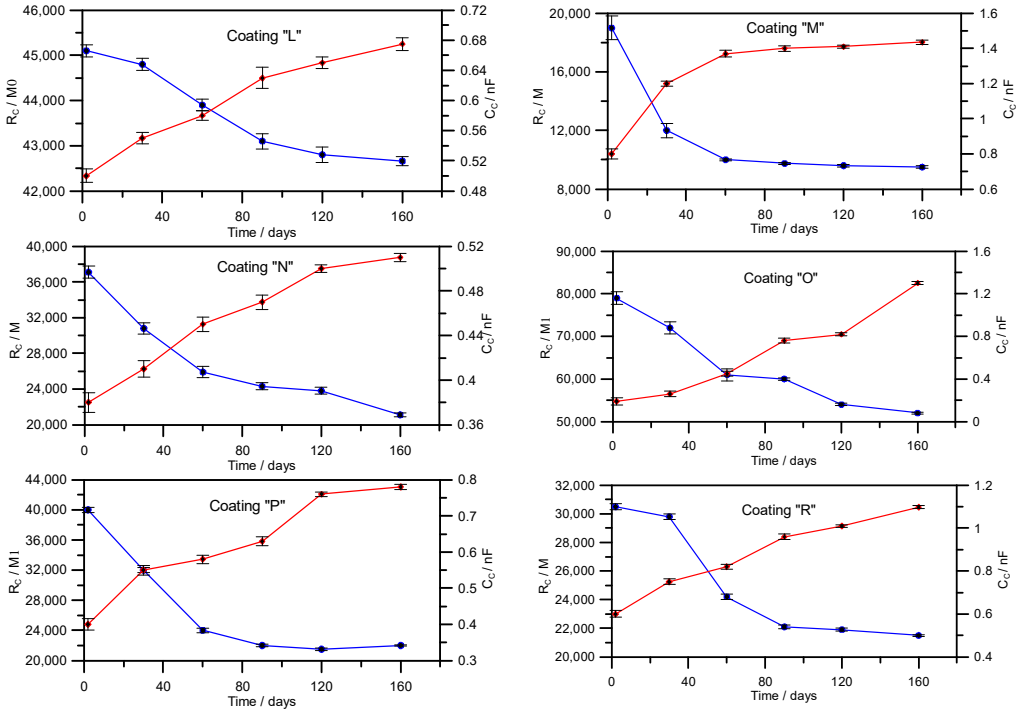

Figure 16. Changes in resistance and capacitance over time obtained for the tested coatings.

The corrosion potential of the steel in the feed ranged from −0.656 to −0.685 V vs. Ag/AgCl depending on the sample. Connecting the potentiostat caused the potential of the steel substrate to drop very quickly to an assumed level of −1.1 V.

At the end of the exposure, a layer of cathodic deposits was found on the surface from which the organic coating had been removed, effectively reducing the surface area polarised during the tests. The plots of the polarising current versus time (Figure 17) show a continuous decrease in the current value. This also demonstrates the lack of negative interaction between cathodic and coating protection, as any loss of adhesion of the coating to the substrate would result in an increase in the current required to polarise the sample. An attempt to mechanically remove the organic coating from the steel surface at the artificial failure boundary also failed. The tested coatings were therefore resistant to environmental alkalisation resulting from the application of cathodic protection.

3.3. Determination of Abrasion Resistance of Wear-Resistant Linings—Industrial Tests

Measurements of the degrees of wear of the spiral-mounted linings were taken according to the points indicated in the sketch below (Figure 18). A view of the linings after exposure is illustrated in Figure 19.

An analysis of the degrees of wear of the tested linings based on the wear measurements shown in Figures 20 and 21 shows that linings made of polyurethane and polymer produced on the basis of MDI and PTMG achieved some of the lowest wear values, which is particularly evident for measurement numbers 4, 5 and 6 (Figure 21).

MOST WIEDZY Downloaded from mostwiedzy.pl

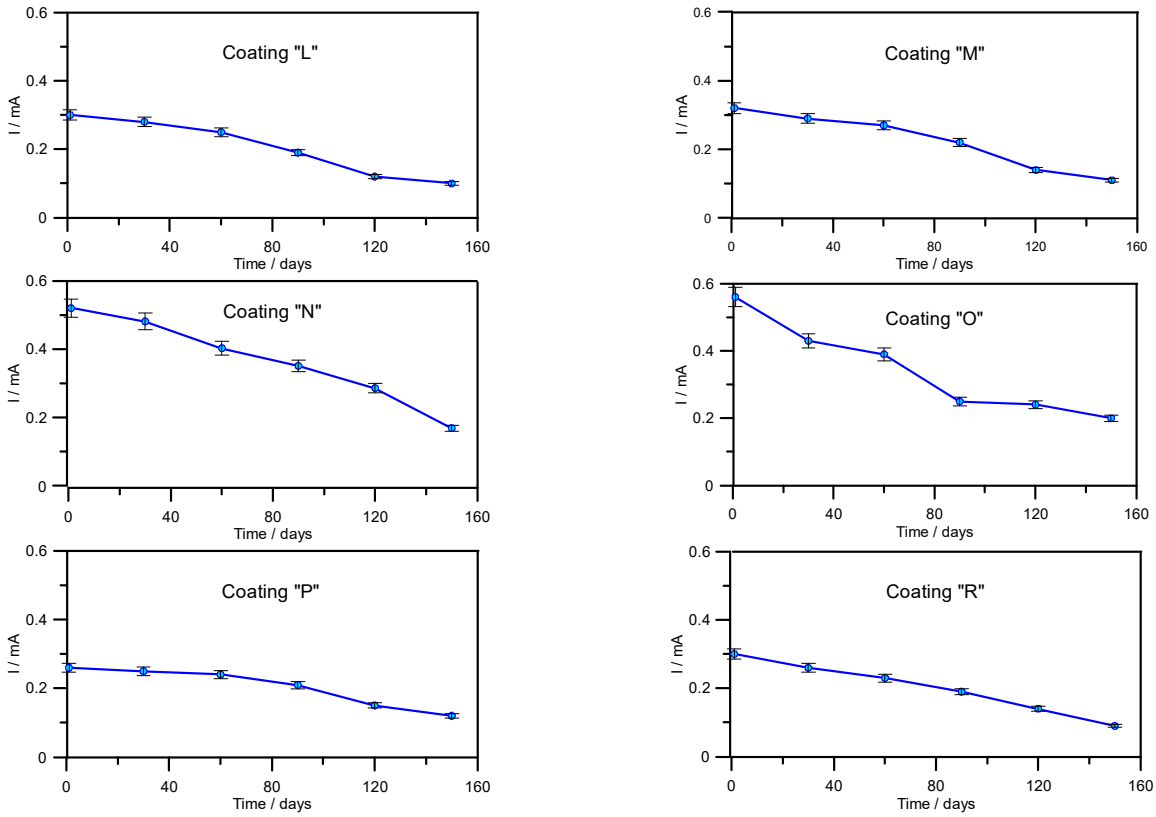

Figure 17. Changes in polarising current during exposure of samples in potentiostatic mode (cathodic protection).

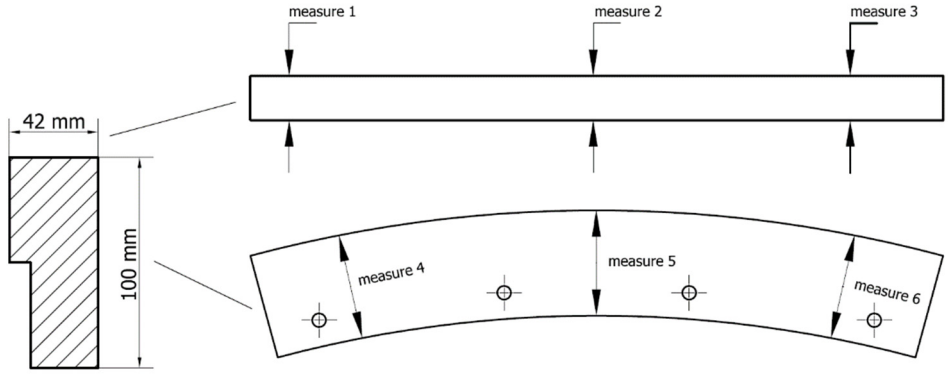

Figure 18. Measurement points for the wear of the classifier lining. Side section (measurements 1, 2 and 3). Frontal part (measurements 4, 5 and 6).

(**a**) (**b**) (**c**)

Figure 19. View of worn linings after the test. (**a**) View of delaminated side surface of polyurethane lining with internal steel core. (**b**) View of worn front surface of high-density polyethylene. (**c**) View of the worn side surface (feed-free side) of PA 6 C (cast polyamide 6).

MOST WIEDZY Downloaded from mostwiedzy.pl

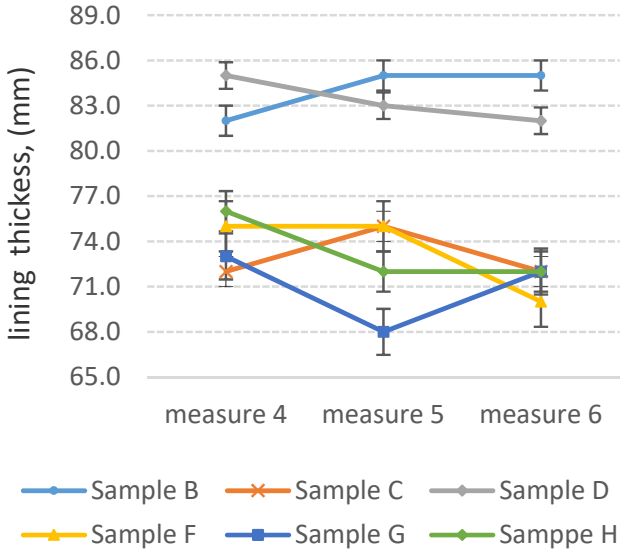

Figure 20. Lining width at three measurement points (side part).

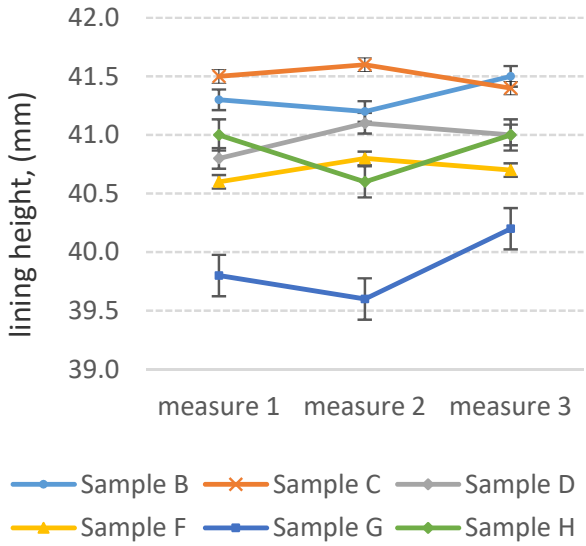

Figure 21. Lining height at three measurement points (front part).

The elastic structure of both materials means that they are able to absorb some of the energy from the pressure force generated by the slurry in the classifier. Additionally noteworthy is the lining made of ultra-high-molecular-weight polyethylene with anti-stick additives, which achieved the lowest wear according to measurement numbers 1 and 2 (Figure 20), which may indicate the low coefficient of friction of this material. The remaining samples achieved a wear (relative to baseline values) above 1 mm for measurements 1, 2 and 3 (Figure 20) and above 23 mm for measurements 4, 5 and 6 (Figure 21).

4. Conclusions

The results obtained showed that it is possible to use industrially applicable materials that will effectively and permanently protect the classifier spiral from corrosive and erosive environments.

Among the linings tested, ultra-high-molecular-weight polyurethanes and polymeric materials achieved the lowest weight losses. In the case of paint coatings, phenolic-epoxy, polyurea-based elastomeric and those containing hard additions of ceramic aggregates

showed the highest durability. All of them showed good barrier properties and resistance to environmental alkalisation resulting from the application of electrochemical protection.

Testing of the linings under industrial conditions confirmed the high erosion resistance of polyurethane and polyethylene-based materials. The optimal solution would be to create a two-material lining consisting of a high-molecular-weight polyethylene with adhesive additives in the front part and a polyurethane or polymeric material in the side part.

During the final selection of paint coatings for the protection of the device, in addition to the abrasion resistance, the possibilities of their cooperation with cathodic protection were taken into account, as well as the weight. As with coatings, the linings used must not exceed the allowable weight, due to the mechanical restrictions mentioned above.

Author Contributions: Conceptualization, methodology, formal analysis and writing—original draft preparation, M.C.; investigation, M.C., K.Z., S.K. (Stefan Krakowiak) and S.K. (Sławomir Kierepa). All authors have read and agreed to the published version of the manuscript.

Funding: This paper originated within a thesis developed in the "Implementation doctorate" programme co-financed from the funds of the Ministry of Science and Higher Education of the Republic of Poland and of KGHM Polska Miedź S.A. at the Department of Electrochemistry, Corrosion and Materials Engineering of the Gdansk University of Technology.

Institutional Review Board Statement: Not applicable.

Informed Consent Statement: Not applicable.

Data Availability Statement: Data sharing is not applicable to this article.

Conflicts of Interest: The authors declare no conflict of interest.

References

1. Bigum, M.; Brogaard, L.; Christensen, T.H. Metal recovery from high-grade WEEE: A life cycle assessment. *J. Hazard. Mater.* **2012**, *207*, 8–14. [CrossRef]
2. Torres, C.M.; Taboada, M.E.; Graber, T.A.; Herreros, O.O.; Ghorbani, Y.; Watling, H.R. The effect of seawater based media on copper dissolution from low-grade copper ore. *Miner. Eng.* **2015**, *71*, 139–145. [CrossRef]
3. Official KGHM Polska Miedź S.A. Site. Available online: https://kghm.com/en/our-business/mining-and-enrichment (accessed on 1 August 2021).
4. Matis, K.A.; Mavros, P. Recovery of metals by ion flotation from dilute aqueous solutions. *Sep. Purif. Methods* **1991**, *20*, 1–48. [CrossRef]
5. Yu, L.; Liu, Q.; Li, S.; Deng, J.; Luo, B.; Lai, H. Adsorption performance of copper ions on arsenopyrite surfaces and implicationsfor flotation. *Appl. Surf. Sci.* **2019**, *488*, 185–193. [CrossRef]
6. Kyzas, G.Z.; Mitropoulos, A.C.; Matis, K.A. From microbubblesto nanobubbles: Effect on flotation. *Processes* **2021**, *9*, 1287. [CrossRef]
7. Sokolović, J.; Stanojlović, R.; Andrić, L.; Stirbanovic, Z.; Ćirić, N. Flotation studies of copper ore Majdanpek to enhance copper recovery and concentrate grade with different collectors. *J. Min. Metall. A Min.* **2019**, *55*, 53–65. [CrossRef]
8. Baran, A.; Śliwka, M.; Lis, M. Selected properties of flotation tailings wastes deposited in the Gilow and Zelazny most waste reservoirs regarding their potential environmental management. *Arch. Min. Sci.* **2013**, *58*, 969–978. [CrossRef]
9. Official KGHM Polska Miedź S.A. Site. Available online: https://kghm.com/en/our-business/processes/ore-enrichment (accessed on 1 August 2021).
10. Skrzypkowski, K.; Korzeniowski, W.; Zagorski, K.; Dudek, P. Application of long expansions rock bolt support in the underground mines of Legnica-Glogow copper district. *Studia Geotechn. Mech.* **2017**, *39*, 45–57. [CrossRef]
11. Biswas, S.; Satapathy, A. A comparative study on erosion characteristics of red mud filled bamboo–epoxy and glass–epoxy composites. *Mater. Des.* **2010**, *31*, 1752–1767. [CrossRef]
12. Duan, C.; Karelin, V.Y. Abrasive erosion and corrosion of hydraulic machinery. *World Sci.* **2003**, *11*, 272. [CrossRef]
13. Ackah, K.; Owusu, C.; Amoah, F. Optimisation of operational parameters of a spiral classifier using design of experiment (DOE). *Ghana Min. J.* **2020**, *20*, 45–50. [CrossRef]
14. Bazin, C.; Sadeghi, M.; Renaud, M. An operational model for a spiral classifier. *Miner. Eng.* **2016**, *91*, 74–85. [CrossRef]
15. Czekajło, M.; Zakowski, K. Failures and a concept of corrosion protectiston system for spiral classifiers at KGHM Polska Miedź S.A. *Ore Conc. Plant. Eng. Fail. Anal.* **2020**, *109*, 104287–104294. [CrossRef]
16. Czekajło, M.; Zakowski, K. Increasing efficiency of technological process by limiting impact of corrosive environment on operation of spiral classifiers. *IOP Conf. Ser. Mater. Sci. Eng.* **2018**, *427*, 012032. [CrossRef]

MOST WIEDZY Downloaded from mostwiedzy.pl

17. Malka, R.; Nešić, S.; Gulino, D.A. Erosion-corrosion and synergistic effects in disturbed liquid-particle flow. *Wear* **2007**, *262*, 791–799. [CrossRef]
18. Atasoy, Y.; Spottiswood, D.J. A study of particle separation in a spiral concentrator. *Miner. Eng.* **1995**, *8*, 1197–1208. [CrossRef]
19. Bazin, C.; Sadeghi, M.; Bourassa, M.; Roy, P.; Lavoie, F.; Cataford, D.; Rochefort, C.; Gosselin, C. Size recovery curves of minerals in industrial spirals for processing iron oxide ores. *Miner. Eng.* **2014**, *65*, 115–123. [CrossRef]
20. Pilov, P.I.; Kirnarsky, A.S. Developments of spiral separation technology for retreatment of fines from coal dumps. Mine planning and equipment section. In *6th International Symposium on Mine Planning and Equipment Selection (MPES)*; Imprint; CRC Press: Ostrava, Czech Republic, 1997; pp. 193–196.
21. Lan, X.; Gao, J.; Du, Y.; Guo, Z. A novel method of selectively enriching and separating rare earth elements from rare-earth concentrate under super gravity. *Miner. Eng.* **2019**, *133*, 27–34. [CrossRef]
22. Altun, N.E.; Sakuhuni, G.; Klein, B. The use of continuous centrifugal gravity concentration in grinding circuit. Modified approach for improved metallurgical performance and reduced grinding requirements. *Physicochem. Probl. Mineral. Pro.* **2015**, *51*, 115–126. [CrossRef]
23. Lu, B.T. Statistical approaches for assessment of water corrosivity. *Corros. Eng. Sci. Technol.* **2011**, *46*, 651–656. [CrossRef]
24. EN ISO 7784-2:2016-05. *Paints and Varnishes—Determination of Resistance to Abrasion—Part 2: Method with Abrasive Rubber Wheels and Rotating Test Specimen*; International Organization for Standardization: Geneva, Switzerland, 2016.
25. EN ISO 2808:2020-01. *Paints and Varnishes—Determination of Film Thickness*; International Organization for Standardization: Geneva, Switzerland, 2019.
26. Zoltán, L.; Tamás, K. A generalized model of the equivalent circuits in the electrochemical impedance spectroscopy. *Electrochim. Acta* **2020**, *363*, 137199. [CrossRef]
27. Margarit-Mattos, I. EIS and organic coatings performance: Revisiting some key points. *Electrochim. Acta* **2020**, *354*, 136725. [CrossRef]
28. Hammouda, N.; Kamel, B. EIS study of the corrosion behavior of an organic coating applied on Algerian oil tanker. *Metall. Res. Technol.* **2020**, *117*, 610. [CrossRef]

MOST WIEDZY Downloaded from mostwiedzy.pl